Journal of *Marine Science and Engineering*

MDPI

Article

Sea State Monitoring by Ship Motion Measurements Onboard a Research Ship in the Antarctic Waters

Silvia Pennino [1,*], Antonio Angrisano [2], Vincenzo Della Corte [3], Giampaolo Ferraioli [1], Salvatore Gaglione [1], Anna Innac [1], Elena Martellato [1], Pasquale Palumbo [1], Vincenzo Piscopo [1], Alessandra Rotundi [1] and Antonio Scamardella [1]

[1] Department of Science and Technology, University of Naples "Parthenope", Centro Direzionale Isola C4, 80143 Naples, Italy; giampaolo.ferraioli@uniparthenope.it (G.F.); salvatore.gaglione@uniparthenope.it (S.G.); anna.innac@uniparthenope.it (A.I.); elena.martellato@uniparthenope.it (E.M.); pasquale.palumbo@uniparthenope.it (P.P.); vincenzo.piscopo@uniparthenope.it (V.P.); alessandra.rotundi@uniparthenope.it (A.R.); antonio.scamardella@uniparthenope.it (A.S.)

[2] University of Benevento "G. Fortunato", Via Raffaele Delcogliano 12, 82100 Benevento, Italy; a.angrisano@unifortunato.eu

[3] IAPS—INAF, Via del Fosso del Cavaliere 100, 00133 Rome, Italy; vincenzo.dellacorte@inaf.it

* Correspondence: silvia.pennino@uniparthenope.it; Tel.: +39-081-547-6686

Abstract: A parametric wave spectrum resembling procedure is applied to detect the sea state parameters, namely the wave peak period and significant wave height, based on the measurement and analysis of the heave and pitch motions of a vessel in a seaway, recorded by a smartphone located onboard the ship. The measurement system makes it possible to determine the heave and pitch acceleration spectra of the reference ship in the encounter frequency domain and, subsequently, the absolute sea spectra once the ship motion transfer functions are provided. The measurements have been carried out onboard the research ship "Laura Bassi", during the oceanographic campaign in the Antarctic Ocean carried out in January and February 2020. The resembled sea spectra are compared with the weather forecast data, provided by the global-WAM (GWAM) model, in order to validate the sea spectrum resembling procedure.

Keywords: wave spectrum resembling procedure; onboard measurements of heave and pitch motions; spectral analysis of ship motions; comparative analysis with weather forecast data

Citation: Pennino, S.; Angrisano, A.; Corte, V.D.; Ferraioli, G.; Gaglione, S.; Innac, A.; Martellato, E.; Palumbo, P.; Piscopo, V.; Rotundi, A.; et al. Sea State Monitoring by Ship Motion Measurements Onboard a Research Ship in the Antarctic Waters. *J. Mar. Sci. Eng.* **2021**, *9*, 64. https://doi.org/10.3390/jmse9010064

Received: 17 December 2020
Accepted: 5 January 2021
Published: 9 January 2021

1. Introduction

The real-time knowledge of sea state conditions, encountered by the ship in a seaway, is useful for different reasons, ranging from the safety of navigation to onboard comfort level. In fact, it provides a decision support system for the master, useful to avoid potentially dangerous phenomena the ship may experience in following and quartering seas, such as surf-riding, broaching, and parametric rolling [1]. It makes it possible to monitor the main seakeeping parameters, connected with the safety of crew [2] and the onboard comfort level experienced by passengers [3]. Finally, it is also useful when the ship voyage is optimized by adaptive weather routing methods, constrained by seakeeping or minimum consumption criteria [4].

The first pioneering works on the assessment of wave spectra, by ship motion measurement and analysis, were carried out in the mid-1970s, with reference to ships without forward speed [5]. In the subsequent years, several attempts were performed to include the Doppler shift, experienced when the ship advances in a seaway [6–8]. Starting from these pioneering works, in the last two decades, special attention was paid to ships advancing in quartering and following seas, as in this case a non-bijective relationship arises between the encounter and absolute frequency domains [9–12]. Additional research activities were carried out to detect the wave spectra by solving a set of equations, involving heave, pitch and

roll motion measurements [13], and to investigate the reliability of resembled sea spectra by means of a comparative analysis with reference hindcast data [14]. Really, most of past research activities were performed in the frequency-domain [15], while only a few studies, mainly based on Kalman filtering, were carried out in the time domain, due to the high numerical effort required to resemble the unknown sea state parameters [16,17]. Finally, Piscopo et al. [18] recently developed a two-step wave spectrum resembling procedure, based on the analysis of heave and pitch motions, which is embodied in current research.

In particular, the wave spectrum procedure is applied to a data set collected onboard the research ship "Laura Bassi" during the oceanographic campaign in the Antarctic Ocean carried out in January and February 2020. In this respect, the main aim of current research is to apply the wave spectrum procedure outlined in Section 2 in a real environment, and validate it against a set of weather forecast data, provided by the global-WAM model.

2. Sea State Monitoring

2.1. Ship Motion Measurements

Ship motions can be efficiently evaluated by low-cost measurement systems, located onboard the vessel and generally placed on the ship symmetry plane, such as common smartphones. In fact, these devices are generally equipped with several built-in sensors, providing raw data with high sample-rate, and belonging to the following main categories, namely: (i) motion sensors, including accelerometers and gyroscopes; (ii) environmental sensors, such as barometers and thermometers; and (iii) position sensors, including magnetometers. All these measurements are generally referred to the local coordinate system depicted in Figure 1a, with their origin at the centre of the touch screen. In addition, apart from these set of built-in sensors, common smartphones are also equipped with a GNSS receiver, which provides the device's position and velocity in a global framework. The reliability of the smartphone's embedded sensors has been preliminary verified and checked through laboratory tests.

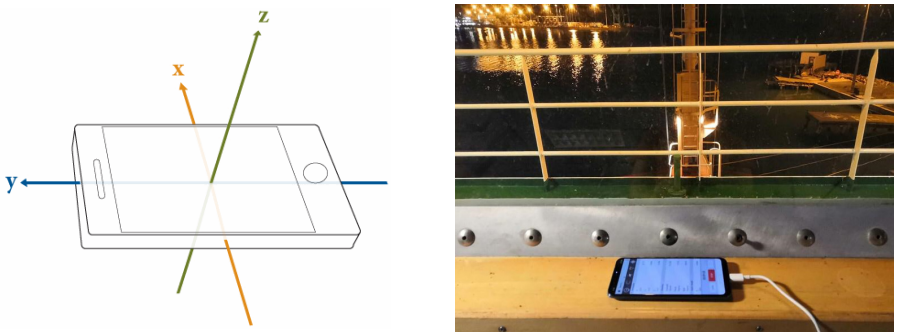

(a) (b)

Figure 1. Coordinates and location of the device: (**a**) system coordinates of the device [19]; (**b**) installation of the device.

In current research, the onboard measurements were performed by the smartphone "Xiaomi Mi 8", located in the wheelhouse on the vertical line passing through the ship centre of mass. The selected location makes it possible to measure the heave acceleration amplitude, with no contribution due to the pitch motion that, in turn, increases among with the longitudinal distance from the vertical line passing though the ship centre of mass. The smartphone was equipped with the module MATLAB® Mobile™, which makes it possible to acquire the data provided by the built-in sensors in the absence of a network connection, with no additional external acquisition systems. In current analysis, orientation and position sensors were embodied, to collect: (i) the ship speed and course; (ii) the device altitude (U); and (iii) the angle between two planes parallel to the touch screen and the ground. Hence, the ship vertical motions between consecutive epochs (k) are computed as in Equation (1):

$$\Delta U_k = U_k - U_{k-1} \quad (1)$$

2.2. Assessment of Weather Forecasting Data

The weather forecast data, embodied in current research to make a comparative analysis possible, with the sea state parameters detected by the ship motion measurements, follow the standardization established by the World Meteorological Organization (WMO), which delivers data in a self-descripting GRIB (Gridded Binary) format [20]. In the current analysis, these data are obtained by the third-generation Global Wave Model (GWAM), initially developed in the mid-1980s by an international group of wave modelers [21], which explicitly solves the wave transport equation with no assumptions about the shape of wave spectra. The model can be applied to both regional and global grids, with arbitrarily set resolution in space and time, based on both latitudinal-longitudinal or Cartesian grids. The model outputs, embodied in the comparative analysis with the resembled sea spectra, are: (i) the significant wave height; (ii) the mean wave period; and (iii) the prevailing direction of the wind wave and swell components.

2.3. Ship Motion Analysis and Wave Spectrum Resembling

The assessment of the sea spectrum in the absolute frequency-domain can be performed once the heave and pitch motion transfer functions in the encounter-frequency domain are provided for both wind wave and swell components. In current analysis, the zero-speed added mass and radiation damping of the research ship "Laura Bassi" are determined by the open-source code NEMOH [22], and subsequently resembled in the encounter-frequency domain, to account for the forward speed [23]. The heading angle between the vessel route and the prevailing wave direction is assumed to be known, thanks to the weather forecast data obtained from the GRIB file, even if it can be in line with the principle monitored by independent systems, such as deployable optic devices, among others. The wave spectrum resembling procedure consists of two subsequent steps [18]. At the first step the wave peak period and the spectrum shape parameter are iteratively varied and detected by a best-fit parametric procedure, which maximizes the non-dimensional parameter provided by Equation (2):

$$\varrho_c\left(T_p^i, \gamma^j\right) = \sqrt{\sum_{k=3,5}\left[\rho\left(\frac{S_{\xi_k}(\boldsymbol{\omega_e})}{\int_0^\infty S_{\xi_k}(\omega_e)d\omega_e}, \frac{|H_k(\boldsymbol{\omega_e})|^2 S_J\left(H_s, T_p^i, \gamma^j, \boldsymbol{\omega_e}\right)}{\int_0^\infty |H_k(\omega_e)|^2 S_J\left(H_s, T_p^i, \gamma^j, \omega_e\right)d\omega_e}\right)\right]^2} \quad (2)$$

where ρ is the Pearson correlation coefficient of heave/pitch motion spectra; S_{ξ_k} and H_k are the heave/pitch (k = 3,5) motion spectrum and transfer function in the encounter-frequency domain and T_p^i and γ^j are the i-th and j-th tentative peak period and shape parameter. The best-fit iterative procedure makes it possible to detect the two unknown parameters or, alternatively, the wave peak period only, if the shape parameter is known, as it occurs for fully developed seas (γ = 1). The number of tentative peak periods and shape parameters is selected to provide an accurate assessment of the unknown variables, paying attention to not excessively increase the time effort amount required to perform the calculations. In this respect, the wave peak period and the shape parameter of the resembled spectrum shall maximize the correlation between heave/pitch theoretical and measured motion spectra, based on the following Equation (3):

$$\left\{T_p^*, \gamma^*\right\} : \varrho_c\left(T_p^*, \gamma^*\right) = max\left(\varrho_c\left(T_p^i, \gamma^j\right)\right) \; \forall (i,j) \epsilon [1,N] \times [1,M] \quad (3)$$

Subsequently, the significant wave height is determined, based on heave, pitch or combined heave/pitch motions, depending on the heave to pitch kinetic energy ratio e assessed by Equation (4):

$$H_s^* = \begin{cases} \frac{\xi_{5,s}}{4\sqrt{\int_0^\infty |H_5(\omega_e)|^2 S_J\left(1,T_p^*,\gamma^*,\omega_e\right)d\omega_e}} & if\ e \le 1/2 \\ \sqrt{\prod_{k=3,5} \frac{\xi_{k,s}}{4\sqrt{\int_0^\infty |H_k(\omega_e)|^2 S_J\left(1,T_p^*,\gamma^*,\omega_e\right)d\omega_e}}} & if\ 1/2 < e < 2 \\ \frac{\xi_{3,s}}{4\sqrt{\int_0^\infty |H_3(\omega_e)|^2 S_J\left(1,T_p^*,\gamma^*,\omega_e\right)d\omega_e}} & if\ e \ge 2 \end{cases} \quad (4)$$

The wave spectrum resembling procedure is tested against sea state conditions characterized by a combination of swell and wind waves, by separating the two contributions and considering them together by evaluating a total component of significant wave height and peak period. The peak periods of swell and wind wave spectra are generally quite different, so it is possible to separate the spectral components due to swell and wind waves, located up to and beyond the so-called separation frequency, respectively, which, in turn, can be efficiently detected based on the only heave motion encounter spectrum by Equation (5):

$$\omega_s : \left.\frac{dS_{\xi_3}(\omega_e)}{d\omega_e}\right|_{\omega_e=\omega_s} = 0 \quad (5)$$

In other words, ω_s almost coincides with the local minimum of the heave motion encounter spectrum, which, in turn, is located between two local maxima, corresponding to the peak frequencies of the swell and wind wave components.

3. Experiment Data

Three data collections, with a 1 Hz sampling rate and 1 h duration, are selected among the data set collected during the voyage of the research ship "Laura Bassi", as detailed in Table 1, where the main data required to perform the analysis are reported. The heave and pitch accelerations of the three data collections are reported in Figure 2a–f, while the acceleration spectra in the encounter wave frequency domain are plotted in Figure 3a–f.

Table 1. Data collection.

Day	Start Point	End Point	Distance (nm)	Heading Angle—Wind (deg)	Heading Angle—Swell (deg)
7 January 2020 13:00–14:00 (local time)	46°19′44.90″ S 173°1′24.13″ E	46°31′5.88″ S 173°1′50.77″ E	11.36	173.63	29.68
8 January 2020 04:00–05:00 (local time)	49°16′14.16″ S 173°4′25.032″ E	49°28′ 35.08″ S 173°3′59.33″ E	12.36	167.35	32.04
14 February 2020 13:21–14:21 (local time)	60°9′20.56″ S 167°4′46.49″ E	59°57′31.14″ S 167°11′37.75″ E	12.32	106.99	78.43

In additon, the main data of the research ship "Laura Bassi", embodied for the scientific activity and logistic support to the Italian Antarctic explorations, are listed in Table 2, while the heave and pitch RAOs (Response Amplitude Operator) are plotted in Figure 4a–f. Finally, the GRIB files have been downloaded on the basis of a 0.25° × 0.25° grid spacing and 3 h forecast interval by means of the free software XyGrib. The distributions of the equivalent significant wave height, defined as the geometric mean of the wind wave and swell components, and the total wave peak period, are reported in Figure 5a–f.

Table 2. Main data of the research ship "Laura Bassi".

Length overall	80.00	m
Length between perpendiculars	72.40	m
Beam on WL	17.00	m
Design draught	6.15	m
Displacement	4736	t
Waterplane area	1074	m^2
Block coefficient	0.599	

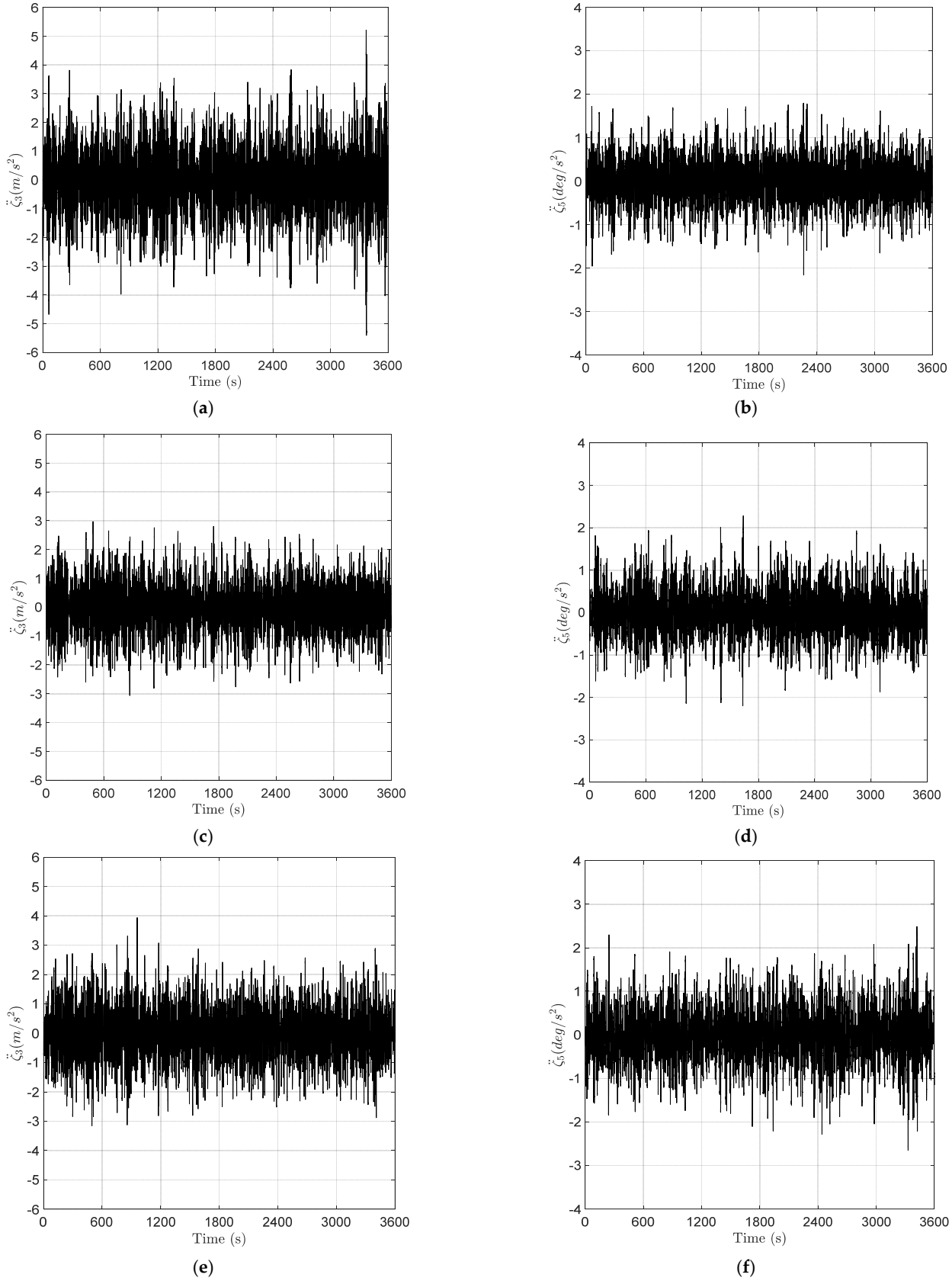

Figure 2. Data collection: (**a**) heave—7 January 2020; (**b**) pitch—7 January 2020; (**c**) heave—8 January 2020; (**d**) pitch—8 January 2020; (**e**) heave—14 February 2020; (**f**) pitch—14 February 2020.

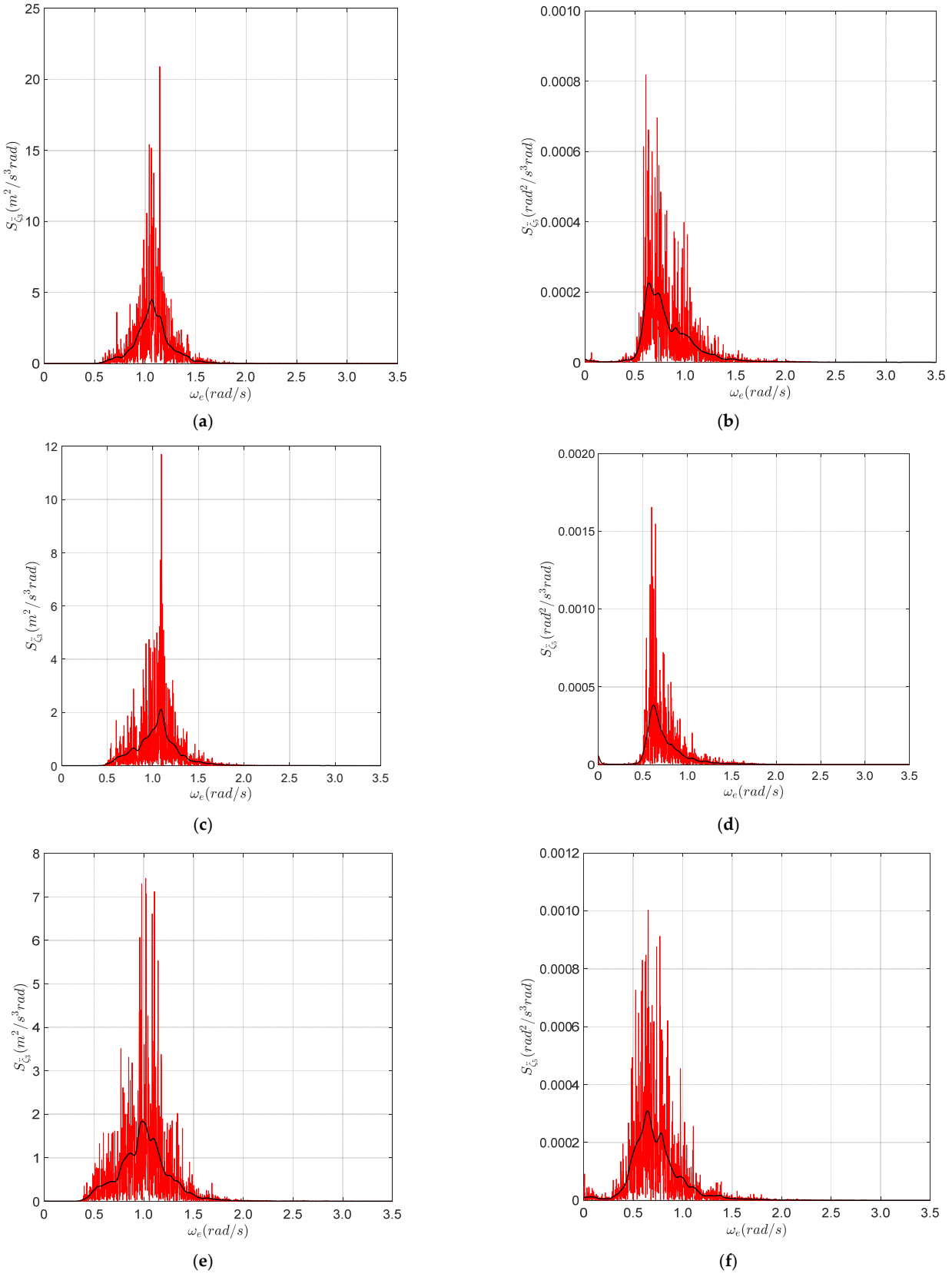

Figure 3. Acceleration spectra in the encounter frequency-domain: (**a**) heave—7 January 2020; (**b**) pitch—7 January 2020; (**c**) heave—8 January 2020; (**d**) pitch—8 January 2020; (**e**) heave—14 February 2020; (**f**) pitch—14 February 2020.

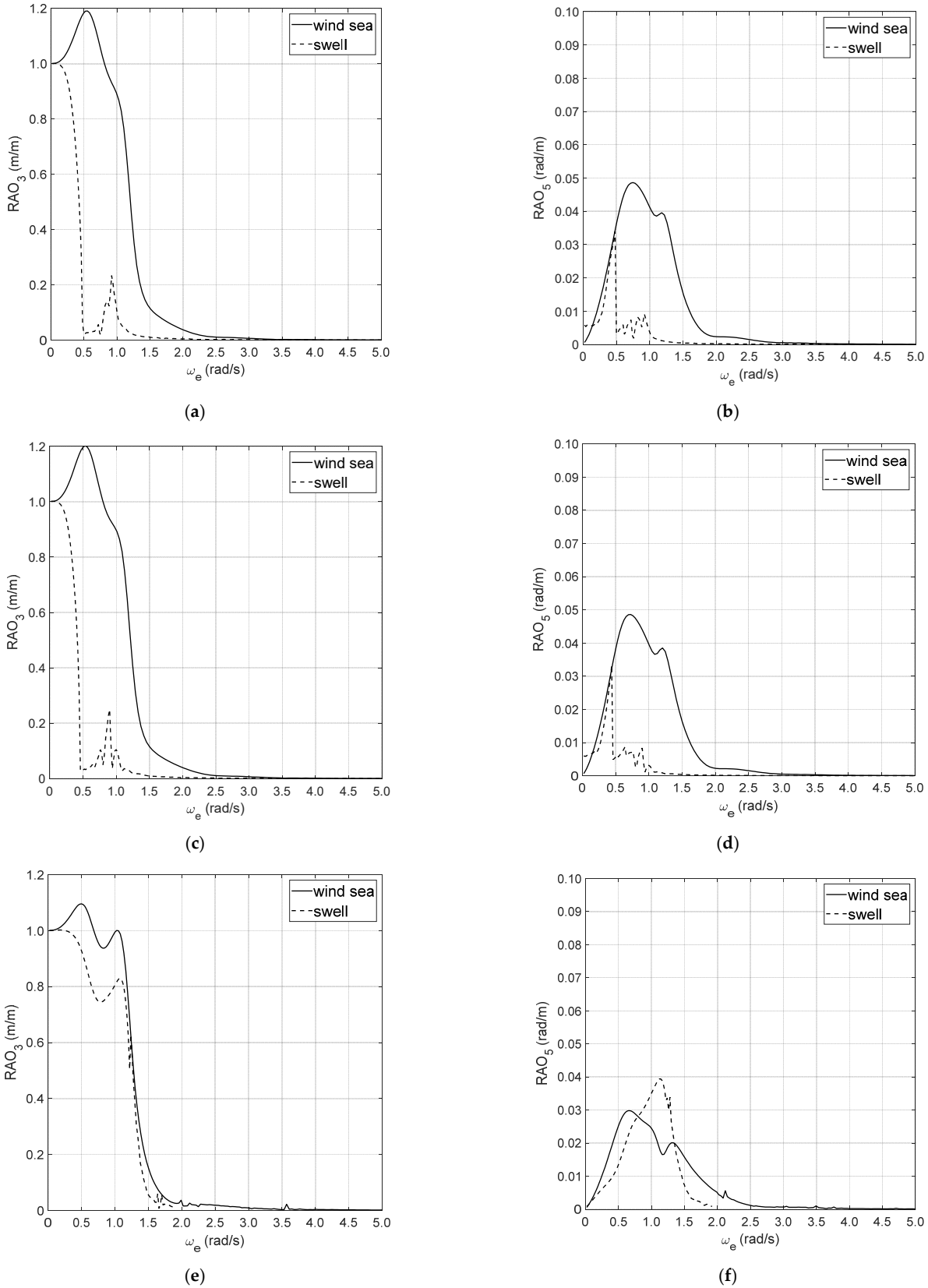

Figure 4. Heave and pitch RAOs (Response Amplitude Operator) in the encounter frequency-domain: (**a**) heave—7 January 2020; (**b**) pitch—7 January 2020; (**c**) heave—8 January 2020; (**d**) pitch—8 January 2020; (**e**) heave—14 February 2020; (**f**) pitch—14 February 2020.

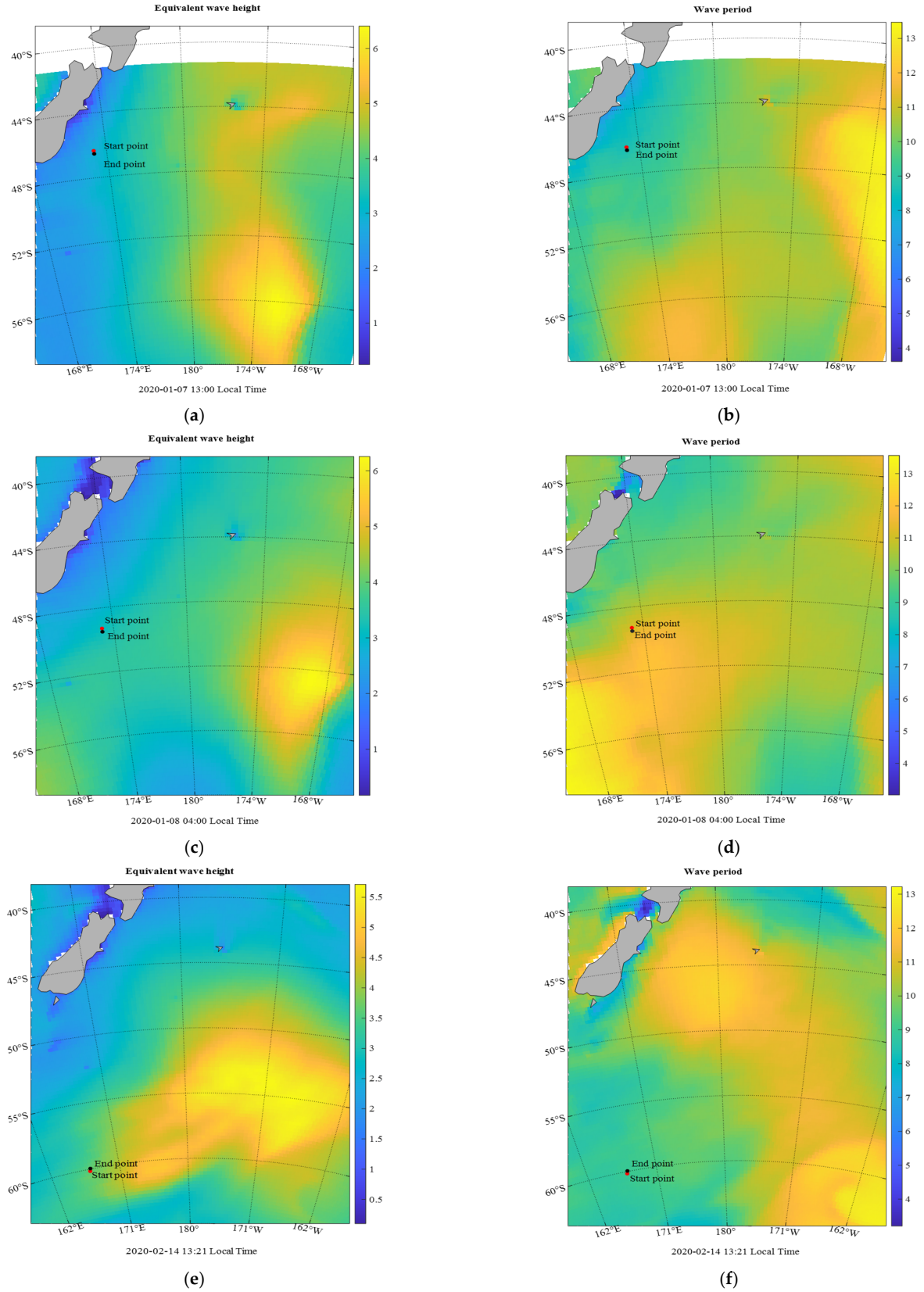

Figure 5. Weather forecast data: (**a**) equivalent wave height—7 January 2020; (**b**) wave period—7 January 2020; (**c**) equivalent wave height—8 January 2020; (**d**) wave period—8 January 2020; (**e**) equivalent wave height—14 February 2020; (**f**) wave period—14 February 2020.

4. Benchmark Study

4.1. First Data Set—7 January 2020

The wave spectrum resembling procedure, described in Section 2.3, is applied to detect the sea state parameters of the three data collections reported in Table 1, based on both heave/pitch motions and accelerations. The results of the first data set are reported in Table 3 and Figure 6a,b, where a comparative analysis with the global wave model Wavewatch III (WWIII) data is performed.

Table 3. Parameters of rebuilt spectrum for a combined sea spectrum—7 January 2020.

	H_S (m)	T_P (s)
Data from WWIII	3.243	12.803
Resembled sea spectrum—motions	3.391 (+4.56%)	11.900 (−7.05%)
Resembled sea spectrum—accelerations	4.360 (+34.44%)	12.900 (+0.75%)

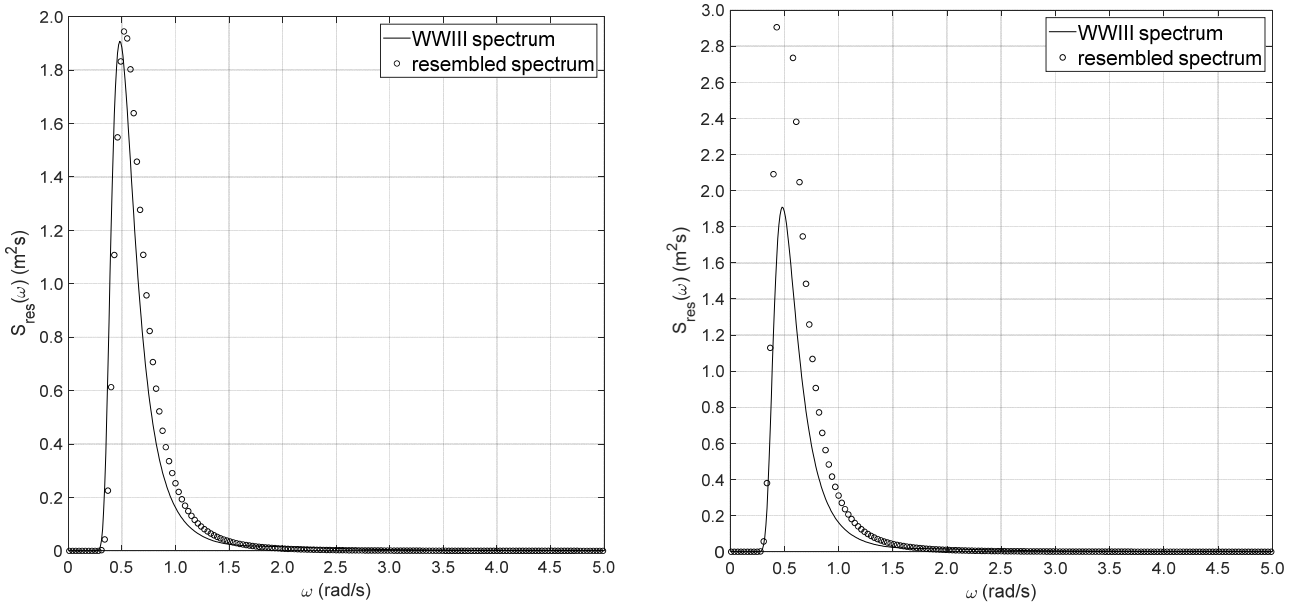

Figure 6. Sea spectrum—7 January 2020: (**a**) resembled combined sea spectrum using heave and pitch motions; (**b**) resembled combined sea spectrum using heave and pitch accelerations.

Based on the current results, the detection of the separation frequency is not possible, so as the wave spectrum reconstruction is performed based on the equivalent wave height due to wind wave and swell components. The sea spectrum reconstruction, based on heave and pitch motion, reveals to be much more effective as regards the other one, based on the ship accelerations, as it can be gathered by the percentage errors as regards the reference WWIII values.

4.2. Second Data Set—8 January 2020

The results concerning the sea spectrum reconstruction of the second data set are reported in Table 4 and in Figure 7a,b. Additionally, in this case, the separation frequency between the wind wave and swell components is not clearly detectable, which implies that the equivalent wave height approach needs to be endorsed. Anyway, despite of the previous reference condition, the sea spectrum reconstruction, based on ship motions and

accelerations, provides almost the same results, with a percentage error which is generally lower than 10%.

Table 4. Parameters of rebuilt spectrum for a combined sea spectrum—8 January 2020.

	H_S (m)	T_P (s)
Data from WWIII	2.576	10.225
Resembled sea spectrum—motions	2.950 (+14.52%)	9.600 (−6.11%)
Resembled sea spectrum—accelerations	2.812 (+9.16%)	11.000 (+7.57%)

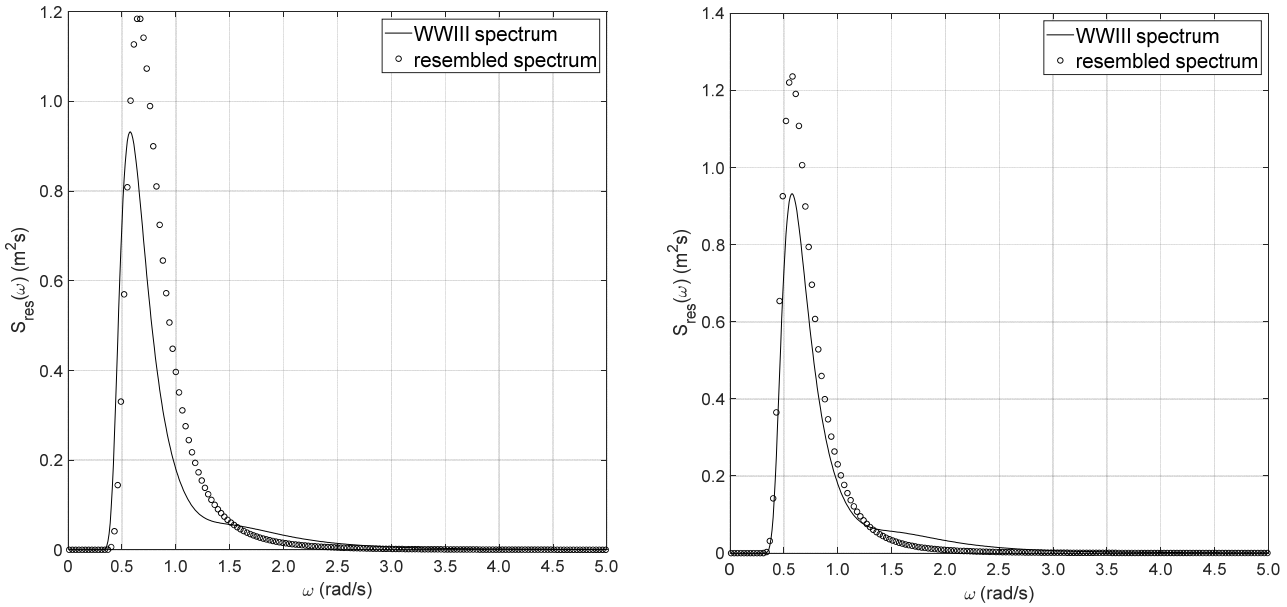

Figure 7. Sea spectrum—8 January 2020: (**a**) resembled combined sea spectrum using heave and pitch motions; (**b**) resembled combined sea spectrum using heave and pitch accelerations.

4.3. Third Data Set—14 February 2020

The results concerning the sea spectrum reconstruction of the last data set are reported in Table 5 and in Figure 8a,b. Additionally, in this case, the separation frequency between the wind wave and swell components is not clearly detectable, which implies that the equivalent wave height approach needs to be endorsed. The sea spectrum reconstruction, based on the ship motion analysis, reveals to be much more effective, as regards the other one, based on the ship accelerations, with reference to the assessment of the significant wave height. Instead, the resembled peak wave periods are almost comparable.

Table 5. Parameters of rebuilt spectrum for a combined sea spectrum—14 February 2020.

	H_S (m)	T_P (s)
Data from WWIII	4.441	9.001
Resembled sea spectrum—motions	4.346 (−2.14%)	9.300 (+3.32%)
Resembled sea spectrum—accelerations	5.167 (+16.34%)	9.400 (+4.43%)

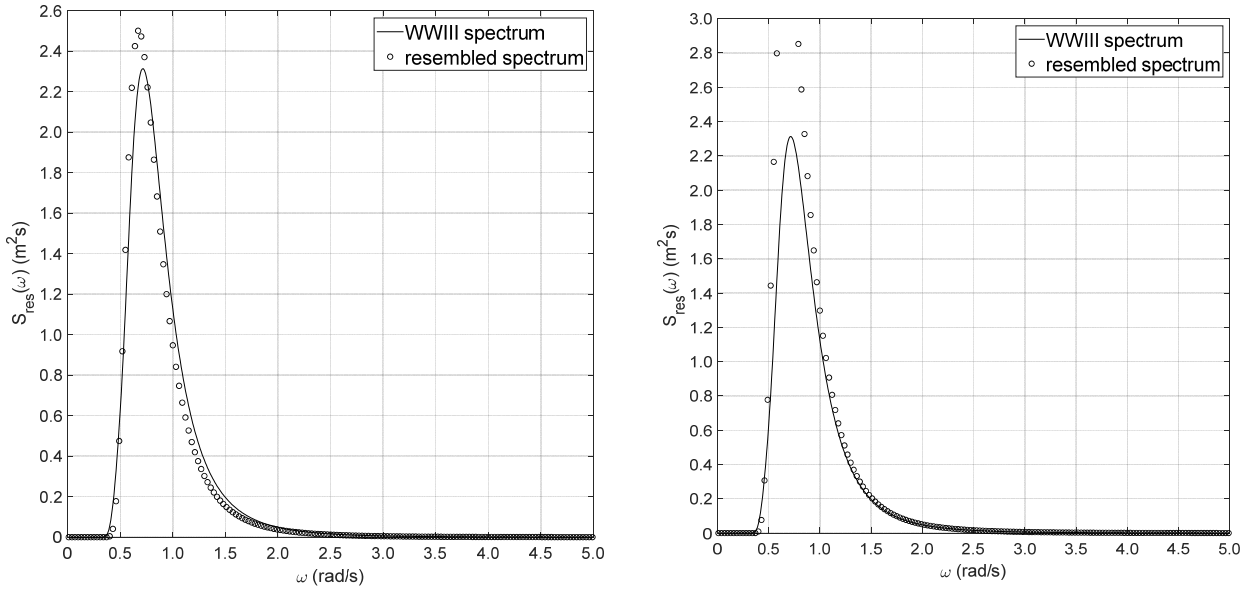

Figure 8. Sea spectrum—14 February 2020: (**a**) resembled combined sea spectrum using heave and pitch motions; (**b**) resembled combined sea spectrum using heave and pitch accelerations.

5. Conclusions

The paper focused on the assessment of the sea state conditions, based on the measurement and analysis of the ship motions and accelerations, recorded onboard the research ship "Laura Bassi" during the oceanographic campaign in the Antarctic Ocean, carried out in January and February 2020. Particularly, three data collections were analyzed by means of the two-step procedure outlined in Section 2.3, and compared with the weather forecast data, provided by the global-WAM model. Based on the results of the benchmark study performed in Section 4, the following main outcomes have been achieved:

- The wave spectrum resembling procedure makes it possible to efficiently assess the sea state parameters, in terms of significant wave height and wave peak period;
- The analysis of ship motions is more effective, as regards the other one based on ship accelerations, to assess the main sea state parameters.

Current outcomes seem to be promising for further developments, mainly devoted to: (i) investigating the possible employment of windowing functions in the Fourier analysis of ship motions and accelerations; (ii) exploring the incidence of time duration on resembled sea state parameters; (iii) comparing the procedure with other resembling procedures. Furthermore, it stands to reason a further improvement in the results for sea states with a more distinct separation between swell and wind waves. These studies will be the subject of future works.

Author Contributions: Conceptualization, S.G., V.P., and A.S.; Writing—original draft, S.P. and A.I.; Writing—review and editing, A.A., S.G., V.P., and A.S.; Methodology, V.P., S.P. and A.I.; Software and formal analysis, V.P., and S.P.; Data curation and visualization, A.A. and A.I.; Supervision, A.A., S.G., V.P., and A.S.; Validation S.G. and V.P.; Funding acquisition, V.D.C., G.F., E.M., P.P., and A.R. All authors have read and agreed to the published version of the manuscript.

Funding: The work was supported by "DORA—Deployable Optics for Remote Sensing Applications" (ARS01_00653), a project funded by MIUR—PON "Research & Innovation"/PNR 2015–2020.

Institutional Review Board Statement: Not applicable.

Informed Consent Statement: Not applicable.

Data Availability Statement: The data presented in this study are available on request from the authors. The data are not publicly available as they have been gathered and treated for the authors.

Acknowledgments: The authors convey a special thanks to Riccardo Scipinotti (Agenzia nazionale per le nuove tecnologie, l'energia e lo sviluppo economico sostenibile—ENEA) and Franco Coren (Istituto Nazionale di Oceanografia e di Geofisica Sperimentale—OGS) for the data and all technical information on the vessel "Laura Bassi".

Conflicts of Interest: The authors declare no conflict of interest.

References

1. Pascoal, R.; Guedes Soares, C.; Sørensen, J. Ocean wave spectral estimation using vessel wave frequency motions. *J. Offshore Mech. Arct. Eng.* **2007**, *129*, 90–96. [CrossRef]
2. Gaglione, S.; Piscopo, V.; Scamardella, A. The overall motion induced interruptions as operability criterion for fishing vessels. *J. Mar. Sci. Technol.* **2016**, *21*, 517–532. [CrossRef]
3. Scamardella, A.; Piscopo, V. Passenger ship seakeeping optimization by the Overall Motion Sickness Incidence. *Ocean Eng.* **2014**, *76*, 86–97. [CrossRef]
4. Pennino, S.; Gaglione, S.; Innac, A.; Piscopo, V.; Scamardella, A. Development of a New Ship Adaptive Weather Routing Model Based on Seakeeping Analysis and Optimization. *J. Mar. Sci. Eng.* **2020**, *8*, 270. [CrossRef]
5. Takekuma, K.; Takahashi, T. On the Evaluation of Sea Spectra Based on the Measured Ship Motions. *Trans. West-Jpn. Soc. Naval Archit.* **1973**, *45*, 51–57.
6. Isobe, M.; Kondo, K.; Horikawa, K. Extension of MLM for Estimating Direction Wave Spectrum. In Proceedings of the Symposium on Description and Modeling of Direction Seas, Danish Hydraulic Institute and Danish Maritime Institute, Copenhagen, Denmark, 18–20 June 1984; Volume A-6.
7. Kobune, K.; Hashimoto, N. Estimation of Directional Spectra from the Maximum Entropy Principle. In Proceedings of the 5th International Offshore Mechanics and Arctic Engineering Symposium (OMAE), Tokyo, Japan, 13–18 April 1986; pp. 80–85.
8. Iseki, T.; Ohtsu, K. Bayesian estimation of directional wave spectra based on ship motions. *Control Eng. Pract.* **2000**, *8*, 215–219.
9. Iseki, T.; Terada, D. Bayesian estimation of direction wave spectra for ship guidance systems. *Int. J. Offshore Pol. Eng.* **2002**, *12*, 25–30.
10. Nielsen, U.D. Estimations of on-site direction wave spectra from measured ship responses. *Mar. Struct.* **2006**, *19*, 33–69. [CrossRef]
11. Nielsen, U.D.; Andersen, I.M.V.; Koning, J. Comparisons of means for estimating sea states from an advancing large containership. In Proceedings of the 12th PRADS, Changwon, Korea, 20–25 October 2013.
12. Montazeri, N.; Nielsen, U.D.; Jensen, J.J. Estimation of wind sea and swell using shipboard measurements—A refined parametric modelling approach. *Appl. Ocean Res.* **2016**, *54*, 73–86. [CrossRef]
13. Brodtkorb, A.H.; Nielsen, U.D.; Sørensen, A. Online wave estimation using vessel motion measurements. In Proceedings of the 11th IFAC Conference on Control Applications in Marine Systems, Robotics, and Vehicles (CAMS), Opatija, Croatia, 10–12 September 2018.
14. Nielsen, U.D.; Diez, J. Ocean wave spectrum estimation using measured vessel motions from an in-service containership. *Mar. Struct.* **2020**, *69*, 102682. [CrossRef]
15. Nielsen, U.D. A concise account of techniques available for shipboard sea state estimation. *Ocean Eng.* **2017**, *129*, 352–362. [CrossRef]
16. Pascoal, R.; Soares, C.G. Kalman filtering of vessel motions for ocean wave directional spectrum estimation. *Ocean Eng.* **2009**, *36*, 477–488. [CrossRef]
17. Pascoal, R.; Perera, L.P.; Soares, C.G. Estimation of directional spectra from ship motions sea trials. *Ocean Eng.* **2017**, *132*, 126–137. [CrossRef]
18. Piscopo, V.; Gaglione, S.; Scamardella, A. A new wave spectrum resembling procedure based on ship motion analysis. *Ocean Eng.* **2020**, *201*, 107137. [CrossRef]
19. Available online: https://se.mathworks.com/help/supportpkg/mobilesensor/ug/phoneorv2.gif (accessed on 26 May 2020).
20. WMO. Introduction to GRIB Edition 1 and GRIB Edition 2. Available online: https://www.wmo.int/pages/prog/www/WMOCodes/Guides/GRIB/Introduction_GRIB1-GRIB2.pdf (accessed on 18 November 2020).
21. Komen, G.J.; Cavaleri, L.; Donelan, M.; Hasselmann, K.; Janssen, P.A.E.M.; Hasselmann, S. *Dynamics and Modelling of Ocean Waves*; Cambridge University Press (CUP): Cambridge, UK, 1994.
22. Salvesen, N.; Tuck, E.O.; Faltinsen, O. Ship motions and sea loads. *SNAME Trans.* **1970**, *6*, 1–30.
23. Babarit, A.; Delhommeau, G. Theoretical and numerical aspects of the open source BEM solver NEMOH. In Proceedings of the 11th European Wave and Tidal Energy Conference, Nantes, France, 6–11 September 2015.